LAWRENCE
LIVERMORE
NATIONAL
LABORATORY

UCRL-TR-210019

Structure and Spectroscopy of Black Hole Accretion Disks

D.A. Liedahl, C.W. Mauche

February 25, 2005

This work was performed under the auspices of the U.S. Department of Energy by University of California, Lawrence Livermore National Laboratory under Contract W-7405-Eng-48.

FY04 LDRD Final Report
Structure and Spectroscopy of Black Hole Accretion Disks
LDRD Project Tracking Code: 02-ERD-004
Duane Liedahl, Principal Investigator

Abstract

The warped spacetime near black holes is one of the most exotic observable environments in the Universe. X-ray spectra from active galaxies obtained with the current generation of X-ray observatories reveal line emission that is modified by both special relativistic and general relativistic effects. The interpretation is that we are witnessing X-ray irradiated matter orbiting in an accretion disk around a supermassive black hole, as it prepares to cross the event horizon. This interpretation, however, is based upon highly schematized models of accretion disk structure. This report describes a project to design a detailed computer model of accretion disk atmospheres, with the goal of elucidating the high radiation density environments associated with mass flows in the curved spacetime near gravitationally collapsed objects. We have evolved the capability to generate realistic theoretical X-ray line spectra of accretion disks, thereby providing the means for a workable exploration of the behavior of matter in the strong-field limit of gravitation.

Project Overview

Black holes, being black, can only be studied through their influence on proximate matter. Nature obliges us in the form of X-ray binaries and active galactic nuclei, where vast quantities of material are available to accrete onto the resident black hole. The discovery of accreting X-ray sources in the 1960s was thus exciting to astrophysicists, who believed that they had found a probe of gravity in the strong-field limit. The optimism was soon quenched, after it was realized that the observed continuum spectra, obtained at low spectral resolving power, could be explained in a number of ways, with or without relativistic effects. The 1990s brought the discovery of iron Kα fluorescence lines (~6.4 keV) from near-neutral gas in the Seyfert 1 galaxy MCG –6-30-15, with profiles that had evidently been skewed by special relativistic beaming and gravitational redshift. So far, approximately 20 extragalactic objects show relativistic line profile deformation. Since line emission provides less ambiguous radiation signatures than continua, the current view is that astronomers now have access to sensitive probes of the spacetime geometry near black holes.

Conservation of angular momentum generally requires accretion to proceed via a disk. As matter proceeds through the disk, it loses gravitational potential energy, which is converted into continuum radiation, much of which lies in the X-ray band. A fraction of these continuum X rays irradiate the disk, a fraction of which is re-radiated in the form of discrete spectral lines, plasma diagnostic signatures of the physical conditions in the disk. Near the black hole, disk material is moving at velocities that are an appreciable fraction of the speed of light. Gravitational redshift and light bending also come into play, further modifying the line spectra. The goal is to solve the inverse problem of inferring the physical structure and kinematic properties of the disk by fitting relativistic disk models to spectroscopic data. The study of line formation near black holes, therefore, entails primarily the interaction of high-energy radiation, propagating through a curved spacetime, with an accretion disk (see Figure 1). Our team has spent the last three years improving the X-ray spectral capabilities of accretion disk models.

In the following sections, we describe the results of our research, including these topics: disk structure, atomic processes, opacity, Monte Carlo photon propagator, and general relativistic effects.

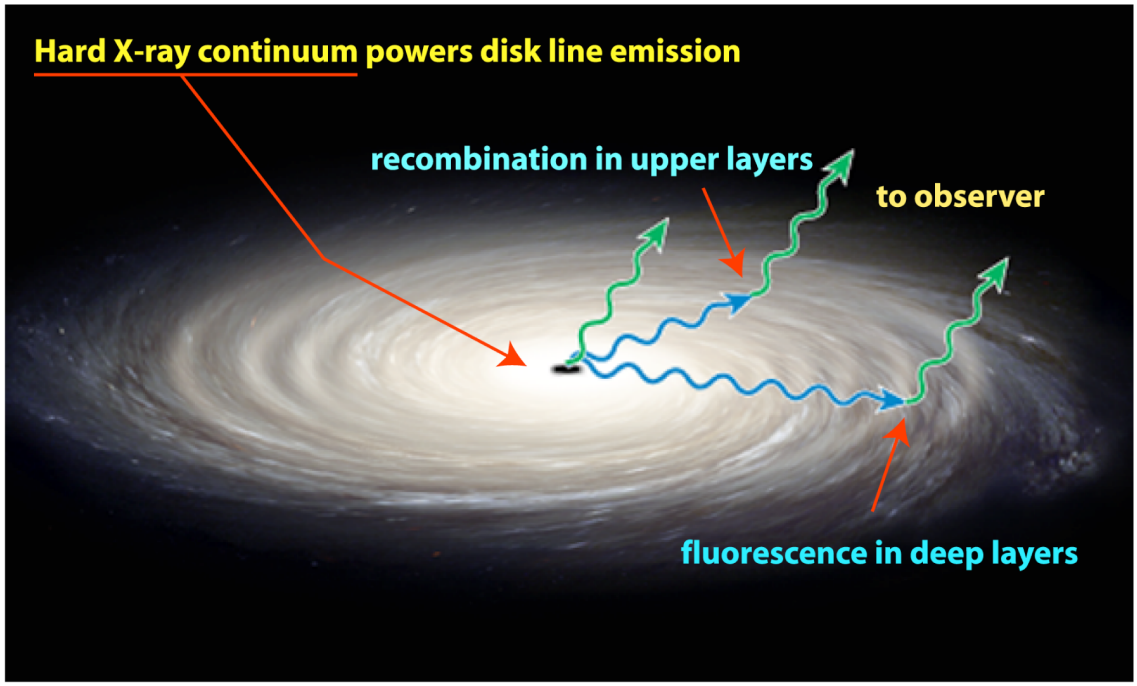

Figure 1. Artist's impression of an accretion disk near a black hole, with a schematic representation of radiation processes relevant to the current study. An intense hard X-ray continuum is generated at small radii just outside the event horizon *(blue arrows)*. Part of the continuum irradiates the disk, producing fluorescence line emission and recombination emission, some which reaches the observer *(green arrows)*.

Results

Disk Structure

The temperature, density, and ionization structure of model disks are described on a two-dimensional coordinate grid, a radial coordinate (r), and a vertical coordinate (z). Our approach is to fix r, to represent a narrow disk annulus, calculate the z structure, choose a new r, calculate the z structure, and so on, thus building up a global model of the disk (see Figure 2). Calculation of the z structure is subject to hydrostatic equilibrium, local thermal balance, and ionization equilibrium. The incident continuum is transferred down through the disk, successively attenuated by the opacity of overlying layers. Solutions to the coupled transfer, energy, and ionization equations are iterated until the hydrostatic condition is satisfied. The emissivity and opacity of each (r,z) gas cell is calculated using the LXSS (Livermore X-ray Spectral Synthesizer) package. Calculations are first performed in the rest frame of a given annulus. Outgoing line and recombination continuum radiation is transferred along lines of sight to the "observer." The outgoing spectrum can be post-processed, in order to account for relativistic effects, such as beaming, gravitational redshift, and light bending. Azimuthal symmetry is assumed, which gives us the full 3-D disk structure.

X-ray irradiated accretion disks are characterized by a steep transition, moving vertically, from a relatively cool (~10^5 K), dense photosphere to a hot, tenuous corona. The temperature jump can be as large as three orders of magnitude, converging to the so-called Compton temperature of roughly 10^8 K at high altitudes. It is inside this transition layer, where temperatures are approximately 10^6 K, that much of the X-ray line emission originates. Specifically, this zone emits recombination radiation. We have refined the calculation of the transition layer. This regime is notoriously difficult owing to the existence of a thermal instability.

We have improved the modeling of the thermally unstable region – or, transition zone – by including convection and conduction.

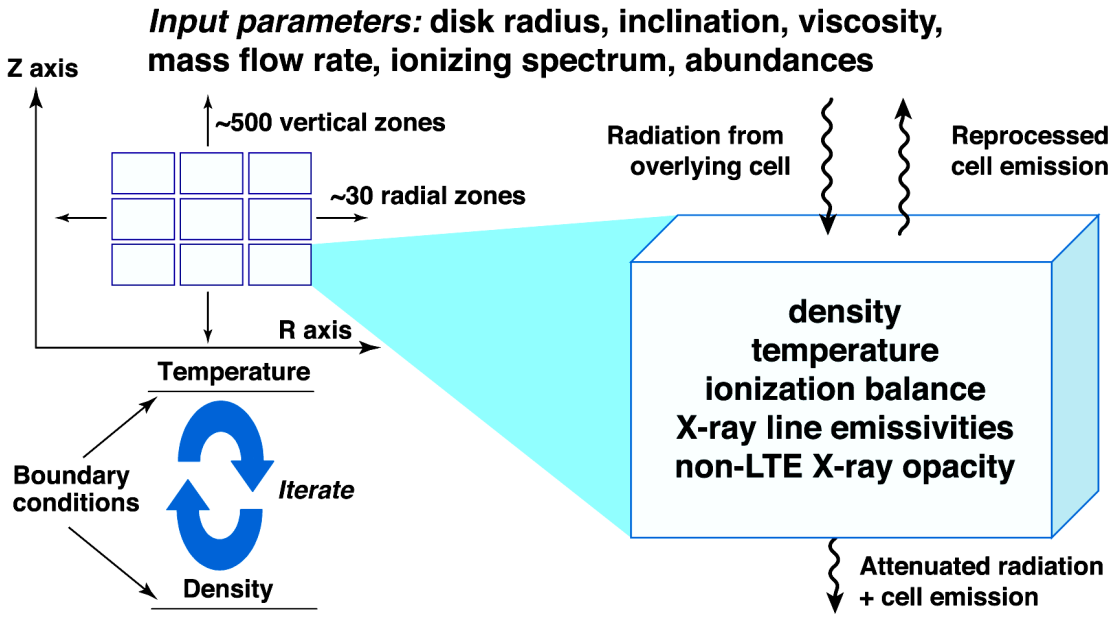

Figure 2. Computational scheme for calculating structure of an accretion disk. For a given set of input parameters, approximately 30 disk atmospheres are calculated, one for each annulus. A lower boundary condition is the particle density, which is specified as a function of radius. An upper boundary condition is the Compton temperature, dictated by the spectral shape of the input continuum. We calculate the plasma and radiative properties of each zone and iterate until the boundary conditions are satisfied, along with thermal balance and hydrostatic equilibrium.

One of the principal aims of this work was to determine the structural – as opposed to spectral – response of the disk to a hard X-ray source. We have discovered and calculated a feedback mechanism that exists between the disk height and the X-ray illumination. Significantly, the disk is found to subtend a solid angle with respect to a point source at the disk center that is larger by an order of magnitude compared to earlier models. The implication of this is that the disk intercepts and reprocesses ten times more radiation than previously thought. This resolves a longstanding problem in accretion disk theory, in which observations in the optical suggested much thicker disks than could be accounted for by current disk theory. Moreover, by iterating on the vertical structure of the disk, finding the correct height dependence of density and temperature, and generating local spectra with our recombination models, we are able to calculate the X-ray spectrum – the essential observable – in a realistic way.

A sample output of the accretion disk code is shown in Figure 3, which shows, in cross-section, contours of line emissivity for four H-like emission lines, superimposed on the *r*-*z* gridding of the model. Note that the spacings in *z* vary, a result dictated by the adaptive mesh refinement scheme employed in the calculation. The grid becomes finer where the temperature or density gradients are steep. The contours are derived from the macrophysics – density, temperature, charge state distributions – and the relevant microphysics – radiative cascade models based upon atomic structure, radiative transition rates, and temperature-dependent recombination rates. Emissivity distributions such as those in the figure constitute the starting point for the Monte Carlo transport code (described below), where the lines, in order to escape to the observer, must traverse the overlying atmospheric layers.

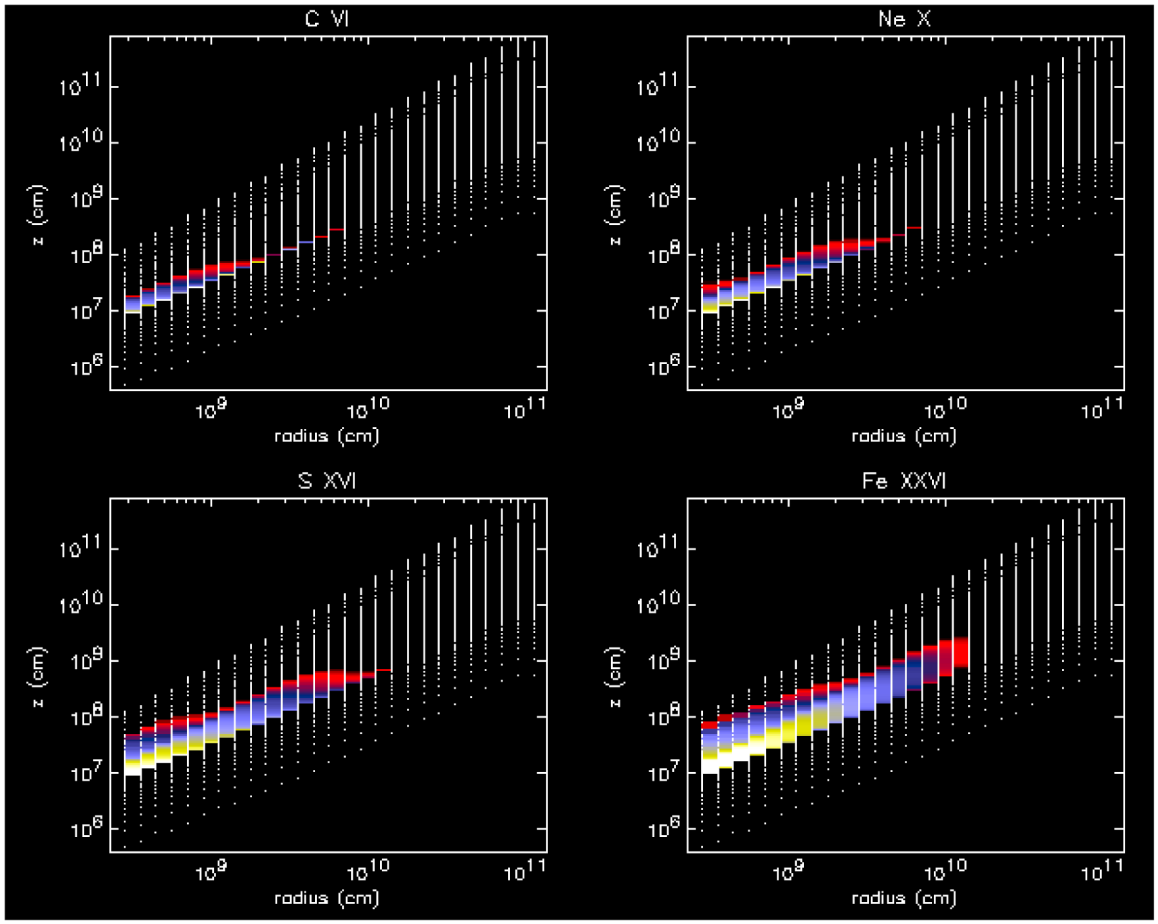

Figure 3. Emission contours for four H-like lines (as labeled). Contours range from white (high) to red (low). This structure is rotated around the *z*-axis, in accordance with the assumption of azimuthal symmetry. This spatial distribution of line emissivity is the starting point for the Monte Carlo transport of line photons from their sites of origin to their sites of destruction or to the observer (see below). Plots show the concentration of emissivity at smaller radii, owing to the higher level of continuum radiation there. The diagonal distribution of atmospheric zones follows the flaring of the disk; the disk scale height increases with radius since the *z*-component of the gravitational field does also.

Atomic Physics

Underlying the large-scale global aspects of the accretion disk problem are complex microphysical processes. The resultant disk structure depends on the small-scale response of plasmas to an external illuminating source. Since the radiation fields are dilute and non-Planckian, and since the electron densities are several orders of magnitude below what would be required to drive the gas into local thermodynamic equilibrium (LTE), each ion species must be treated according to a detailed level accounting scheme, wherein level populations are calculated explicitly, based upon a tally of all rates into and out of each atomic energy level. This requires careful treatments of photoionization, photoexcitation, recombination, collisional excitation, radiative cascades, and autoionization.

Spectra of X-ray photoionized gases in cosmic settings are somewhat unique in that X-ray emission from *all* charge states of the abundant elements heavier than helium can appear in spectroscopic data from a given celestial source. Recombination emission is characteristic of high charge states, and is thus characteristic of the upper atmosphere. Our atomic recombination emission database includes carbon, nitrogen, oxygen, neon, magnesium, silicon, sulfur, argon, calcium, and iron. Figure 4 is a sample output

spectrum from a disk structure calculation, showing the recombination spectrum over the range 1-35 Å. The broad features are recombination continua, and can be quite prominent in X-ray photoionized plasmas owing to the high degree of overionization.

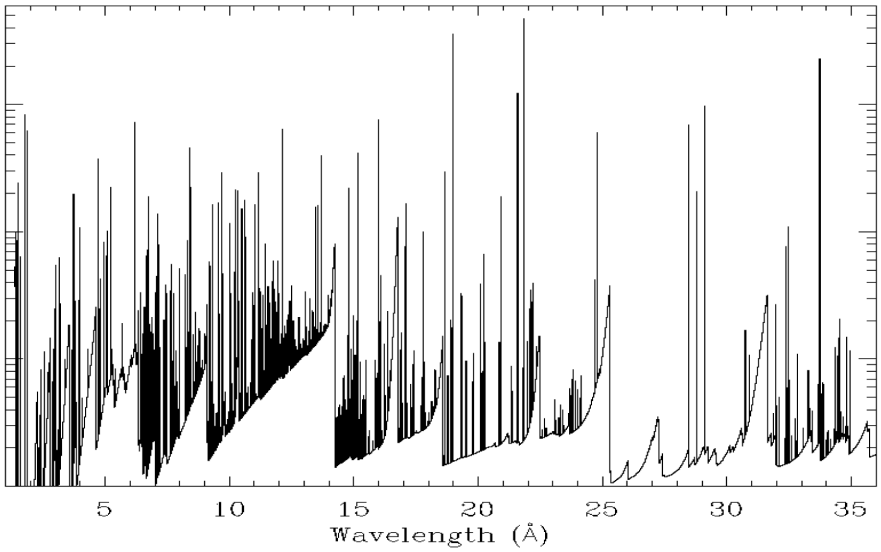

Figure 4. Model spectrum based upon calculation of accretion disk atmospheric structure. Discrete spectrum is dominated by recombination cascades in H-like and He-like ions. Broad features are recombination continua, formed by transitions of continuum electrons to the ground configurations of these same ions.

Fluorescence emission arises predominantly from lower charge states. Its presence in X-ray spectra signifies hard X-ray irradiation of fairly cold, near-neutral matter. This matter resides in deep layers of the accretion disk, below the transition region. In these layers, matter resists valence shell photoionization, owing to the attenuation of the soft X-ray and ultraviolet flux by overlying material. Only hard X-rays have the penetrating power to reach these layers. For X-ray photons with energies above ~10 keV, Compton scattering is the dominant photon/particle interaction. However, some fraction of the hard X-ray photons will be absorbed by the K edges of elements retaining K-shell electrons. This leads to fluorescence emission, caused by the radiative decay of autoionizing energy levels.

Observations of relativistically distorted iron fluorescence emission led to the realization that there exists an unambiguous (at least, in principle) spectroscopic probe of curved spacetime in the strong-field limit. The key word is, perhaps, *unambiguous*. While much hinges upon these probes, little work is being done in the field to understand them at the microphysical level. We are exploiting our atomic modeling capability to bring the requisite atomic physics up to a level commensurate with what is required of it, viz., to serve as unambiguous probes of extremely hostile, little explored, environments.

We have developed large-scale atomic models of iron and silicon that can be used to study their Kα (i.e., n=2 to n=1 radiative transitions) fluorescence spectra in great detail. While current atomic models reduce the Kα spectrum of each ion to exactly two features, Kα$_1$ and Kα$_2$, we calculate the entire spectrum, which can consist of several hundred lines. This has particular importance for the radiative transfer of the Kα complex. The transfer process is known as resonant Auger destruction, and has, in past research, been shown, in principle, to be crucial to the understanding of fluorescence spectra from an X-ray irradiated plasma. Briefly, resonant Auger destruction occurs when a Kα photon is absorbed by the same transition in another (but identical) ion, and the resultant autoionizing level decays through electron ejection (the Auger effect) rather than by radiative decay. Since fluorescence yields for low-to-mid-Z elements are fairly low,

resonant Auger destruction is an efficient suppressor of Kα photons when line optical depths are of order unity or above. We have studied the ion-to-ion variation of the "zero-D" fluorescence spectrum, as well as the differential effects of resonant Auger destruction, and find that we can use the results to constrain geometric and physical models of X-ray irradiated plasmas in accretion-powered objects, and especially, in black hole accretion disks.

In Figure 5, we show a relatively simple example of the effect of resonant Auger destruction. The figure shows Li-like iron for four different absorbing column densities. The spectra are generated by calculating the inner-shell photoionization rates for all significantly populated energy levels of Be-like iron, which leads to the creation of autoionizing energy levels in the Li-like charge state. Calculation of line fluorescent yields, i.e., the radiative decay probabilities to all allowed lower levels, then gives the spectrum shown in the upper left panel – the zero-D spectrum. Using an escape probability method based on Voigt line profiles, we then subject the lines generated in zero-D to various absorbing column densities. As can be seen in the remaining three panels of Figure 5, we find a surprisingly complex spectral response, even for this simple 3-electron ion. We point out that it has been the practice of other research groups to simply "zero out" Kα lines of the Li-like through Ne-like charge states, assuming that resonant Auger destruction would quench all lines from these ions. For this range of column densities, clearly, such an assumption leads to an underestimate of the Kα line flux. Moreover, with such an assumption, one sacrifices the potential diagnostic utility of these ions.

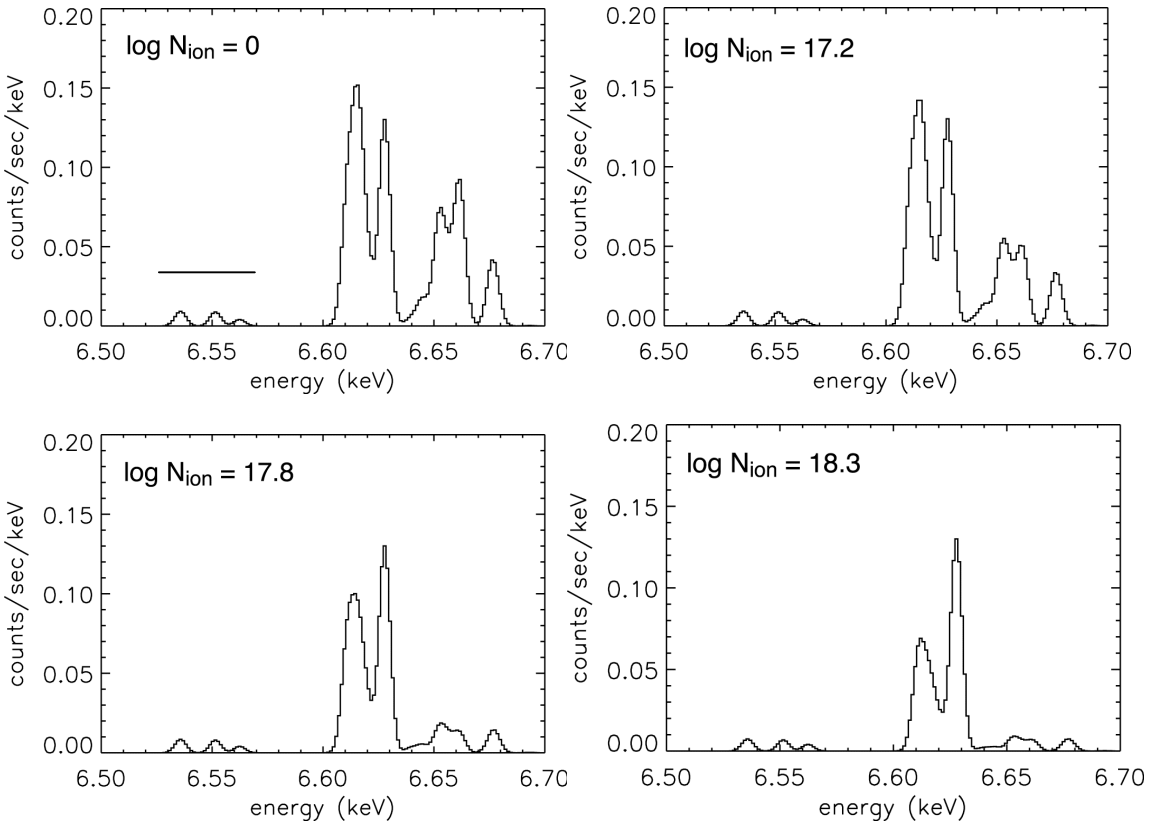

Figure 5. Model spectra of Li-like iron, illustrating the selective action of resonant Auger destruction in modifying the spectra relative to an optically thin (zero-D) plasma. The horizontal line in the top left panel indicates the lines that standard atomic models predict. Units of column density are cm^{-2}. Models are convolved with a gaussian resolution kernel with FWHM = 6 eV.

Non-LTE Opacity

The downward passage of ionizing radiation through the disk atmosphere is mediated by the opacity. Also, discrete emission produced as a by-product of radiation reprocessing is subject to scattering, splitting, or destruction, which again, is determined by the opacity. Since plasma in the disk atmosphere is not in local thermodynamic equilibrium (LTE), the density and temperature dependence of the opacity must be explicitly considered. We calculate the sum of three kinds of opacity: photoelectric, discrete, and electron scattering.

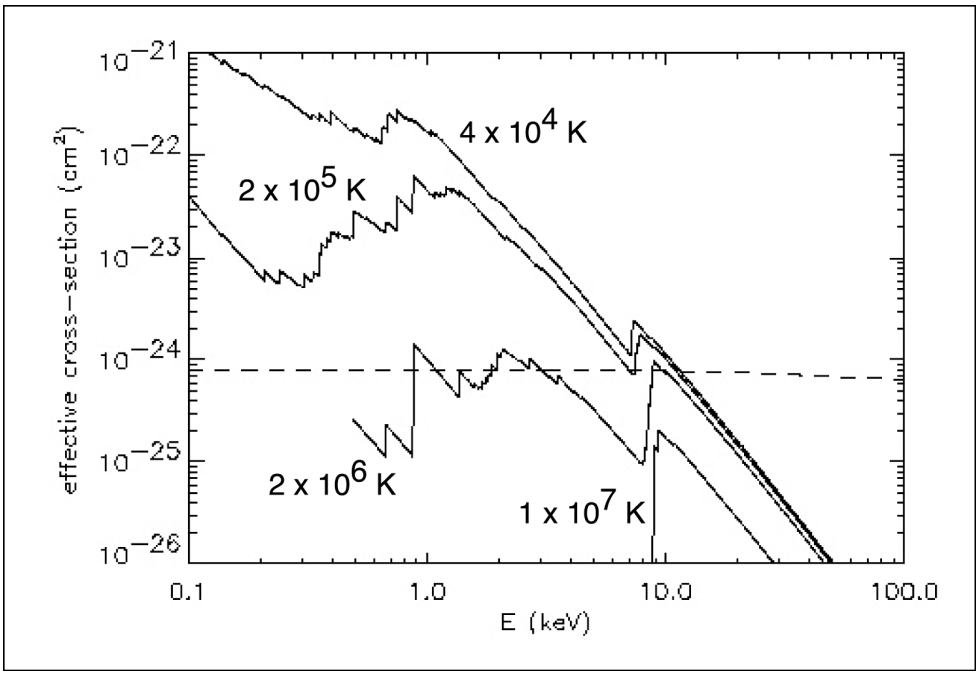

Figure 6. Photoelectric cross-section vs. photon energy for four electron temperatures, based upon the charge state distribution as calculated by the disk structure code, and based upon an assumed chemical abundance distribution. The dashed line shows the baseline Compton cross-section. The slight downturn in the Compton cross-section moving to high energies shows the trend as given by the Klein-Nishina relativistic cross-section. Plots show the rapid drop in cross-section as the temperature increases, beginning at low energies, owing to the successively greater stripping of bound electrons. Photoelectric cross-sections are from Verner & Yakovlev (1995).

For the photoelectric opacity (see Figure 6), we use cross-sections specific to each non-relativistic subshell, which will be modified to account for "*j*-splitting" according to the statistical weight distributions. These atomic data have been extracted from a paper by Verner & Yakovlev (1995). For the time being, we prefer these cross-sections over those that we can generate using an internal code (PIC), owing to the fact that the high-energy behavior of the cross-sections compiled by the former appears to be better behaved than in the latter. In particular, PIC cross-sections tend to drastically overestimate the true cross-sections at energies several times threshold, which, in turn, leads to overestimates of the continuum opacity. We believe that this arises not from fundamental problems with the physics contained in PIC, but that it is simply an artifact of the relatively narrow range over which the fitting formulae are valid. We would need to extrapolate these PIC cross-sections to outside their range of validity, so have opted for the Verner & Yakovlev compilation.

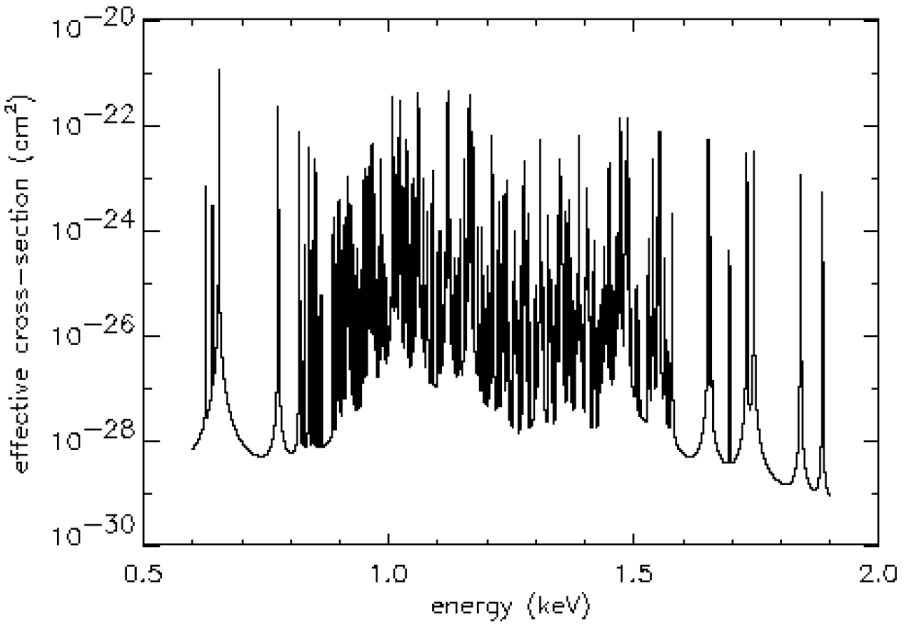

Figure 7. Cross-sections from discrete transitions at 2 million degrees K, assuming Voigt line profiles. The dominant agents of opacity in this spectral range are L-shell ions of iron.

Line opacity is less straightforward than photoelectric opacity. We are in the process of upgrading the disk structure code by adding detailed line opacities calculated with the Hebrew University/Lawrence Livermore Atomic Code (HULLAC), which is one of the workhorses in PAT. In addition, we will incorporate line scattering into the Monte Carlo code. With HULLAC, we calculate the atomic structure, radiative transition rates, including the four lowest multipoles, and, where needed, autoionization rates. We assume Voigt profiles. The local net line opacity is calculated as a superposition of those from individual transitions, summed over all charge states, then over all elements, according to the local temperature density, charge state distribution, and chemical abundance distribution. This involves tens of thousands of lines, and can be exceptionally complex (see Figure 7), depending on the conditions and the spectral band under consideration. As in the case of emission lines discussed above, we are uniquely capable in this area. When complete, our non-LTE opacity model will be unmatched outside of LLNL.

During FY02, we have completed most of the atomic database required for this purpose. We have calculated atomic data for all transitions between bound, stabilized levels for all charge states of carbon, nitrogen, oxygen, neon, magnesium, silicon, sulfur, argon, calcium, iron, and nickel. We have written a subroutine to process this data, and generate effective cross-sections on an energy grid. Implementation will follow.

Monte Carlo Photon Propagation Simulator

The second part of COMPASS is the Monte Carlo (MC) code, which has been designed to follow photons through the pre-calculated black hole environment, from their source to the boundaries of the computational space. In this sense, the MC code is a post-processor to the structure code. The practice of "splitting" the problem – disk first, photons second – calls for some justification. The structure physics is dominated by the radiation flow of the continuum and its interaction with matter through photoelectric and discrete absorption. This can be handled accurately by the disk code, since it includes a good continuum opacity model and a discrete opacity model that is being advanced to the state of the art, as described in Section 2. By-products of radiation reprocessing, such as continuum deformation through Compton scattering, or generation of discrete emission, have a relatively small impact on the disk physics. Therefore, we are justified in relegating a careful treatment of radiation reprocessing to the MC domain. This is

especially important for emission lines. While emission lines do not substantially affect the disk structure, the converse is not true. Emission lines are the observational signatures most sensitive to disk structure and dynamics. This provides the motivation for the MC approach.

Work to date has resulted in a MC code with the following capabilities:

- exact relativistic treatment of Comptonization effects by Maxwellian electron distribution of arbitrary temperature for discrete radiation
- exact relativistic treatment of Comptonization effects by Maxwellian electron distribution of arbitrary temperature for continuum radiation of arbitrary spectral shape
- probabilistically weighted photoelectric absorption by 168 charge states of 13 elements
- fluorescence emission from K shells of 11 elements probabilistically weighted according to fluorescence yields
- simulation of transmission and/or reflection spectra for multi-zone plasmas of arbitrary density structure, temperature structure, and ionization distribution

The MC electron scattering code can accommodate multi-zone propagation, which allow inclusion of gradients in temperature and density, and can deal with velocity fields and gradients.

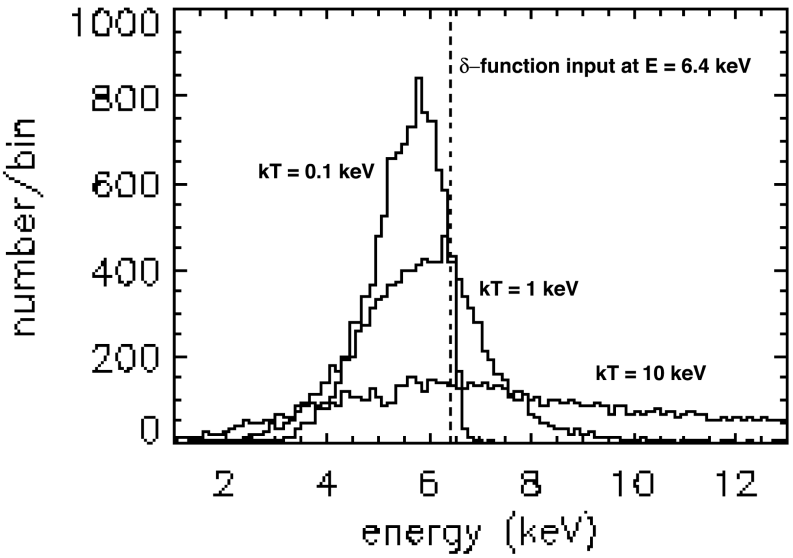

Figure 8. Monte Carlo simulations of relativistic Compton scattering of 6.4 keV δ-function emission line off Maxwellian-distributed electron population for three temperatures, as shown. Photon source is set at the center of an isothermal sphere with Thomson depth 5.

Single-zone simulations were the bread and butter of work performed in this field during the 1990s. Typically, however, that work did not include a proper treatment of Compton scattering of emission lines, as we do, but rather assumed a cold gas, where Compton scattering reduces to pure electron recoil in the observer frame. Moreover, the scattering angle distribution was usually treated as though it were isotropic or, at best, as though it could be adequately described by the Thomson differential cross-section. Thus the angular distributions were calculated incorrectly. In our treatment, we first transform to the electron rest frame by a sequence of coordinate rotations and a Lorentz transform, where the electron's momentum four-

vector is drawn randomly, weighted according to a Maxwellian probability distribution. A Maxwellian distribution adequately describes the electron distribution, since we will rarely find need to model temperatures above 10^8 K. The photon's momentum four-vector is identically transformed. Further coordinate rotations transform the working coordinate system so as to place the *z*-axis along the photon's propagation vector. The scattering angles are calculated in this frame randomly, weighted according to the fully relativistic Klein-Nishina differential cross-section, and the electron recoil is determined. Inverse transformations re-assign a momentum four-vector for the outgoing photon in the fixed observer frame. A typical scatter involves 14 random numbers drawn from six distinct probability distributions.

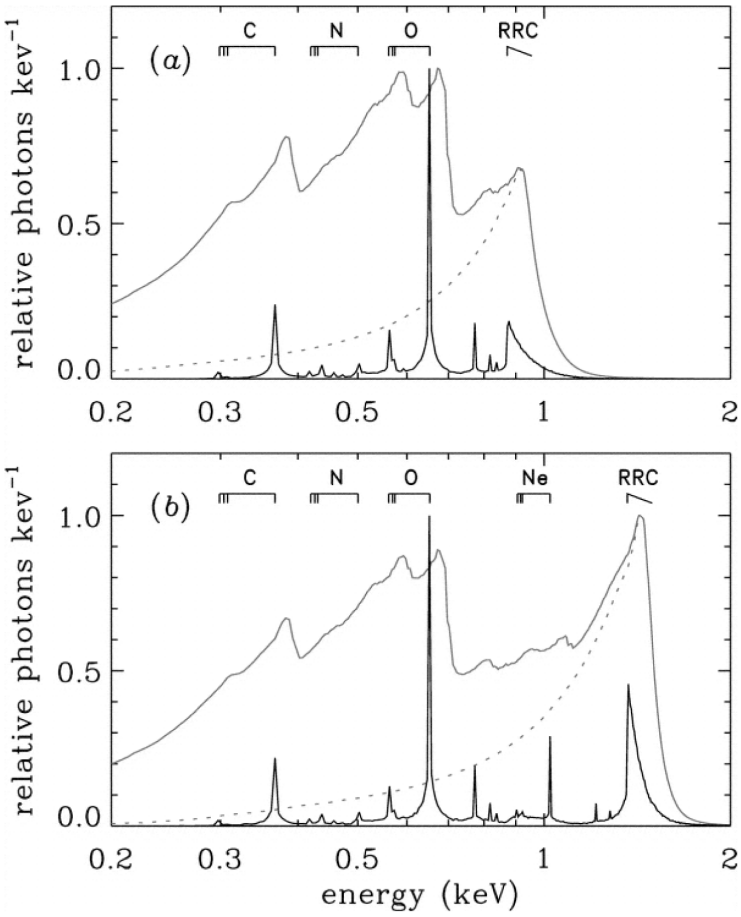

Figure 9. Monte Carlo calculation of radiation reprocessing in a black hole accretion disk. These two examples illustrate the fate of recombination continuum (RRC) emission from H-like oxygen *(top)* and H-like neon *(bottom)*. The H-like oxygen run begins with the RRC feature near 0.9 keV, with an pre-calculated emissivity distribution throughout the disk similar to those shown in Figure 3. A series of photoelectric absorptions and Compton scatters tends to degrade the flux to lower energies, i.e., photoabsorption followed by recombination produces "daughter" photons of lower energy. The daughters are then followed from the reprocessing site, and they may also suffer an energy degradation. The result – the escaping flux – is a series of lines and continua with energies below the original RRC distribution. In this way, emission line fluxes are either enhanced or reduced by radiation transport through the disk. The gray-colored line shows the escaping flux as modified by relativistic effects. The gray-colored dotted line shows the result absent radiation transport. The result for the H-like neon RRC (1.4 keV) is similar.

An example of the MC scattering code output is provided in Figure 8. The calculation assumes a monochromatic (6.4 keV) photon source located at the center of an isothermal sphere of Thomson depth 5. Three runs are shown, each at a different temperature, as indicated. The sensitivity to the electron temperature is obvious. Note the predominant redshift of the line at the two lower temperatures. This effect shows that proper modeling of Compton scattering is crucial in order to avoid confusion between Compton processes and relativistic effects, such as gravitational redshift (see below). At the highest of the three temperatures, the line nearly loses its identity, as its flux is spread across a broad energy range. Separating such a broadened feature from the underlying photoionizing continuum would pose a significant problem for analysts. Thus these results show the sensitivity of lines to atmospheric Compton scattering.

The addition of photoelectric opacity to the MC code has enhanced its capability by allowing for photon conversion and destruction. By "conversion," we refer to the process of creating an ion in an excited state by means of inner-shell photoionization that subsequently relaxes through characteristic photon emission. We define "destruction" as the removal of a photon from our consideration, owing to a series of conversions that downgrades its energy to one below the range of interest, or owing to its migration to substantial depths in the atmosphere from which the probability of escape is negligible. An additional destruction criterion has been added – if the photon wanders across the event horizon, it is decidedly removed from our consideration. The mix of photon destruction and Compton scattering has allowed us to model the processes of reflection and transmission. The reflection phenomenon is an essential process in black hole accretion disks, where a hard X-ray source of continuum radiation impinges upon a plasma. With the development of multi-zone capability, we will thereafter dispense with the slab geometry, and implement the accretion disk model, which is concave structurally, and is rich in physical gradients.

Using the Monte Carlo code, we investigated the radiation transfer of Lyman alpha, helium alpha, and recombination continua in carbon, nitrogen, oxygen, and neon in the photoionized atmosphere of a relativistic black hole accretion disk (Mauche et al. 2004). We found that photoelectric opacity causes significant attenuation of photons with energies above the O VIII K-edge; that the conversion efficiencies of these photons into lower-energy lines are high; and that accounting for this reprocessing significantly increases the flux of X-ray lines from carbon and oxygen escaping the disk atmosphere (see Figure 9). These findings bear on the recent controversies associated with the interpretations of *Chandra* and *XMM* data from supermassive black holes.

Relativistic Effects

Among the unique aspects of COMPASS will be its ability to track photon trajectories through a *matter-filled* curved spacetime. By contrast, other researchers have restricted their calculations to ray tracing in vacuum, with little regard for the physical nature of the photon source, let alone atomic-scale interactions of these photons with the black hole exterior environment. For our purposes, the general relativistic effects of interest are gravitational redshift and the bending of light trajectories.

Solutions to the Einstein field equations for the spacetime metric in the vicinity of a massive object yield two physically viable metrics – the Schwarzschild solution and the Kerr solution. The former is the simpler of the two, and applies to a non-rotating black hole. The metric is spherically symmetric, and is parameterized by the mass alone. The latter applies to a rotating black hole. The metric is cylindrically symmetric, and is more realistic, since the initial collapse of a massive star to form the hole must conserve angular momentum. The Kerr solution is known exactly, and can be described as a family of two-parameter (mass and angular momentum) metrics. In the limit of zero black hole angular momentum, it reduces to the Schwarzschild solution.

There are relativistic effects pertaining to the high velocities encountered in accretion disks near black holes, i.e., special relativistic effects. Velocities near 0.5c are typical. Thus transformation from the disk frame to the observer frame require Lorentz transformations to yield the relativistic Doppler effect. Also, because of the way angles transform under Lorentz transformations, relativistic beaming (sometimes called *the headlight effect*) is an important process. In fact, in tracking photons from cell to cell, Lorentz

transformations appropriate to the relative motion of the cells must be included before we can calculation the interaction physics in the frame of a particular cell.

Figure 10 helps to illustrate a few of the relativistic effects that COMPASS models. Start with an emission line with energy E_o produced in the rest frame of a cell (black in Figure 10). Imagine a narrow annulus surrounding the black hole at a radius $R=6GM/c^2$, and let the ring rotate at the velocity corresponding to a circular orbit at that radius ($0.5c$). View this rotating ring near edge-on. A Newtonian analysis of the resulting line shape would account for the relative velocity of each element of the ring with respect to an observer at rest near the ring. According to the Newtonian version of the Doppler effect, the green curve would be observed. Notice that it is symmetric with respect to the rest frame energy (E/E_o=1)An application of the relativistic Doppler effect and relativistic beaming would change the distribution of the line to that shown in blue. Note that the blue-shifted component of the line appears brighter than the red-shifted component, an illustration of the headlight effect. Finally, we apply the gravitational redshift to the feature, resulting in the red curve. The importance of relativity can be appreciated by comparing the red curve to the green curve.

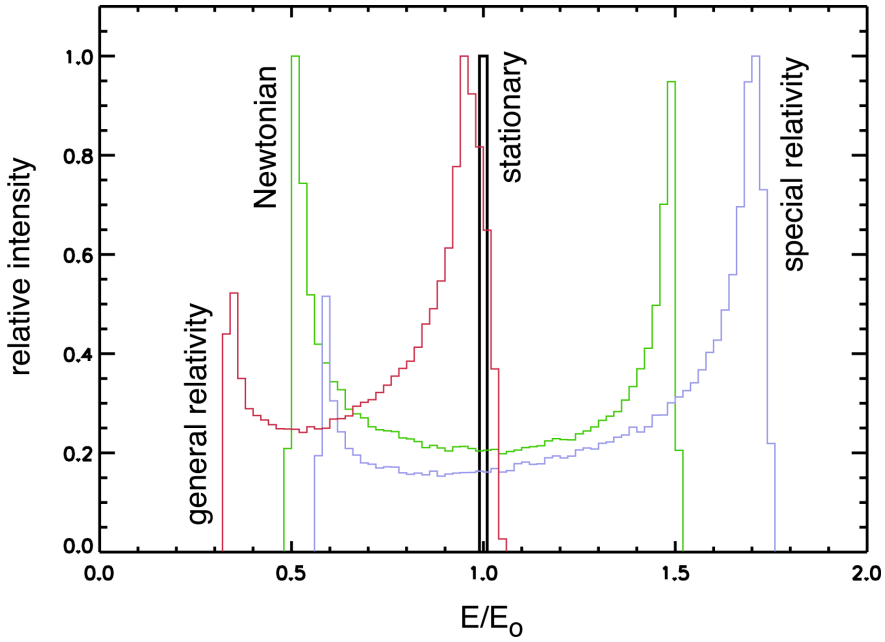

Figure 10. Illustration of the observed distortions of an emission line emitted in a rotating ring near a black hole after being subjected to various relativistic corrections (see text). The Newtonian result can be compared with the relativistic result by comparing the green and red curves.

Another general relativistic effect is known as light bending. As measured by distant observers, photons do not move along straight lines through curved spacetime. Photon paths are obtained by solving the equations of motion for massless particles, which provide trajectories known as geodesics. Geodesics in the Kerr metric can be extremely complex, and will easily defy one's intuition. Perhaps the most peculiar effect on the spacetime surrounding a Kerr black hole is inertial frame dragging, which can be visualized by calculating the trajectory of a photon launched toward the center of the hole from a large distance. According to an observer at "infinity," the photon will appear to acquire angular momentum (although it starts with none) and go into orbit around the hole, gradually spiraling its way through the event horizon (see Figure 11). The event horizon itself is collapsed relative to that for a non-rotating hole, which permits the observation of radiation from regions with a correspondingly larger curvature and greater particle velocities than for the non-spinning case. These aspects lead to the possibility of using radiation signatures

to probe the specific form of the metric, which may lead to a better understanding of black hole formation, for example.

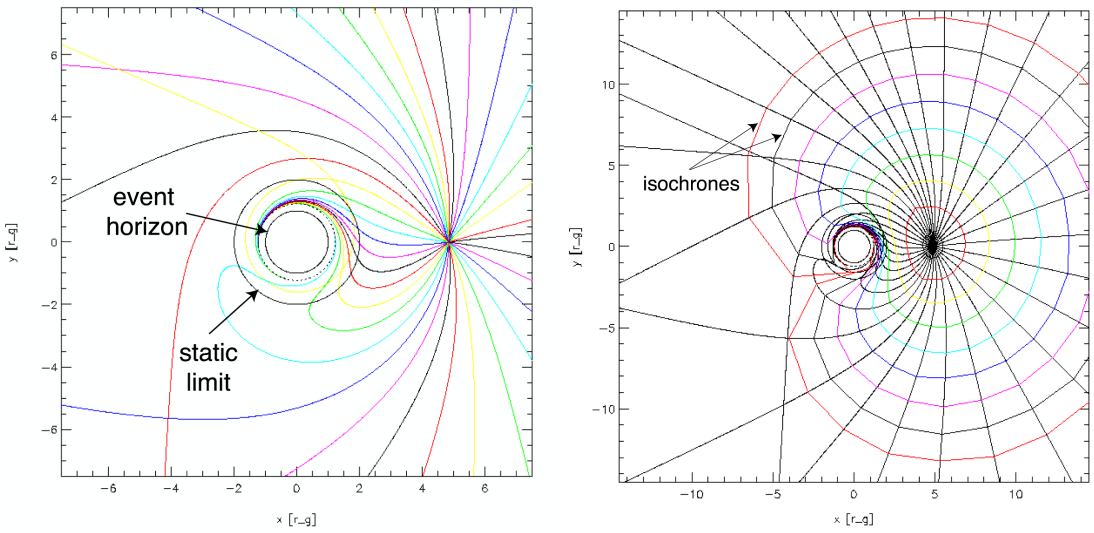

Figure 11. *(Left panel)* Photon trajectories in the equatorial plane of a maximally spinning (counterclockwise) black hole, with the source located at a distance of $5R_g$. The black hole center is at (0,0); the event horizon and static limit are indicated. Once a photon crosses the static limit, it cannot, according to a distant observer, move in the direction opposite to the black hole spin. *(Right panel)* Similar to the left panel, except that isochrones (surfaces of constant time according to a distant observer) are superimposed. The isochrones track the time dependence of the photon trajectories. Deviations from perfect spheres (circles in cross-section) indicate that the speed of light appears to slow as a wavefront approaches the black hole.

We are currently in the process of upgrading the Monte Carlo code to simulate trajectories in the Kerr metric. First, however, we will test a geodesic solver for the Schwarzschild metric. Solutions in the Schwarzschild metric are the *lingua franca* of black hole research, since, owing to its spherical symmetry, this metric is vastly simpler. By exploiting certain constants of the motion, geodesics can be described exactly by a first-order differential equation. Therefore, it is relatively straightforward, and we can perform simplified simulations that can be compared to earlier work, thereby providing assurance that we are correctly implementing geodesic ray tracing. By contrast, trajectories in the Kerr metric are described by two second-order differential equations, which couple the polar and radial coordinates. Considerable care must be applied in treating the initial conditions at the photon launching point, and the initial conditions must be reset after each photon/particle interaction. A Kerr geodesic solver is currently in hand, and we will fully integrate this capability into the Monte Carlo propagator once it has been thoroughly tested.

Exit Plan

This work has applications relevant to research and observation in high-energy astrophysics, especially X-ray astronomy, where the currently deployed *Chandra* and *XMM-Newton* X-ray observatories are returning spectroscopic data from black hole systems. Moreover, *Astro-E2* is scheduled for launch in Summer 2005. With its high-resolution X-ray calorimeter, which is optimized for spectroscopic observations near the iron K lines, black hole systems will be among the priorities for this mission. The next major U.S. X-ray observatory, *Constellation-X*, has as its primary science driver the study of relativistically modified X-ray line emission near black holes. Our long-range plan is to exploit the need for believable accretion disk spectral models that has been engendered by the data returned by the aforementioned satellites. There are

NASA theory programs, as well as the Long Term Space Astrophysics Program, that can fund the research described here. We can increase our chances of securing funding by first publishing at least two more papers in refereed journals, such as *The Astrophysical Journal*. Proposal submissions for FY06 are tenable, given our current schedule and level of progress.

Acknowledgements

The authors acknowledge the other members of the COMPASS team – Mario Jimenez-Garate, John Raymond, Benjamin Mathiesen, and Vijay Sonnad.

References

Verner, D.A., & Yakovlev, D.G. 1995, *A&A Suppl. Ser*., 109, 125.

Project-related Papers

Jimenez-Garate, M., Raymond, and Liedahl, D.A. 2002, "The Structure and X-ray Recombination Emission of a Centrally Illuminated Accretion Disk Atmosphere and Corona," *The Astrophysical Journal*, 581, 1297

Mauche, C.W., Liedahl, D.A., Mathiesen, B.F., Jimenez-Garate, M.A., and Raymond, J.C. 2004, "Reprocessing of Soft X-ray Emission Lines in Black Hole Accretion Disks," *The Astrophysical Journal,* 606, 168

Jimenez-Garate, M.A., Liedahl, D.A., Mauche, C.W., and Raymond, J.C. 2005, "Atomic X-ray Spectra of Accretion Disk Atmospheres in the Kerr Metric," in *Proceedings of the 10th Marcel Grossman Meeting on General Relativity*, World Scientific, Rio de Janeiro, July, 2003, in press

Jimenez-Garate, M.A., Raymond, J.C., Mauche, C.W., and Liedahl, D.A. 2005, "Structure and High-Resolution X-ray Spectrum of a Hydrostatic Accretion Disk Around a Kerr Black Hole," *The Astrophysical Journal* (in press)

Liedahl, D.A. 2005, "Resonant Auger Destruction and Iron Kα Spectra in Compact X-ray Sources," X-ray Diagnostics of Astrophysical Plasmas, Cambridge, MA, November, 2004, (American Institute of Physics), in press.

Liedahl, D.A. 2005, "Iron Kα Spectra from an Atomic Modeling Perspective," Atomic Data for X-ray Astronomy, 25th Meeting of the IAU, Joint Discussion 17, 22 July 2003, Sydney, to appear in *PASP*.

Invited Talks

Mauche, C.W., Constellation-X Spectroscopy Workshop, June, 2003, New York City.
Liedahl, D.A., 25th Meeting of the IAU, Joint Discussion 17, July 2003, Sydney Australia.
Liedahl, D.A., X-ray Diagnostics for Astrophysics, November, 2004, Cambridge, MA.
Jimenez-Garate, M.A., X-ray Diagnostics for Astrophysics, November, 2004, Cambridge, MA.
Liedahl, D.A., Spectra and Timing of Accreting X-ray Binaries, January, 2005, Bombay, India.

Miscellaneous

Poster presentation: American Astronomical Society Meeting, 2003, *"Accretion Disk Atmospheres Around Kerr Black Holes,"* M. Jimenez-Garate, C. Mauche, D. Liedahl, J. Raymond, B. Mathiesen.

Poster presentation: Constellation-X Spectroscopy Workshop, 2003, *"X-ray Spectroscopy of Black Hole Accretion Disk Atmospheres,"* M. Jimenez-Garate, C. Mauche, D. Liedahl, J. Raymond.

Poster presentation: 10th Marcel Grossman Meeting on General Relativity, 2003, *"X-ray Spectroscopy of Black Hole Accretion Disk Atmospheres,"* M. Jimenez-Garate, C. Mauche, D. Liedahl, J. Raymond.

Poster presentation: American Astronomical Society HEAD meeting, 2004, *"A Monte Carlo Treatment of Radiation Transfer in Black Hole Accretion Disks,"* C. Mauche, D. Liedahl, M. Jimenez-Garate.

Description of project to be included in S&TR (2005) commemorating Einstein centennial year.

Paper in preparation by D. Liedahl and D. Torres – working title "Atomic X-ray Spectroscopy as a Probe of Curved Spacetime," one of twelve Einstein Centennial Review Articles, published in *Canadian Journal of Physics* (2005).